FEDERICA POMPA – federica.pompa@subatech.in2p3.fr

In collaboration with M. Martínez-Vara, J. Martín-Albo, M. Sorel

Dark Matter and Neutrinos – 20/05/2025

ADVANCED RECONSTRUCTION CAPABILITIES OF XENON TPC FOR NEUTRINOLESS DOUBLE-BETA DECAY SEARCHES

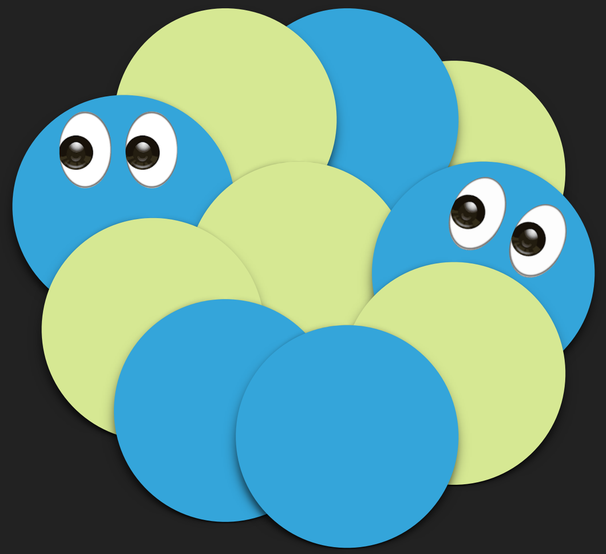

(A, Z)

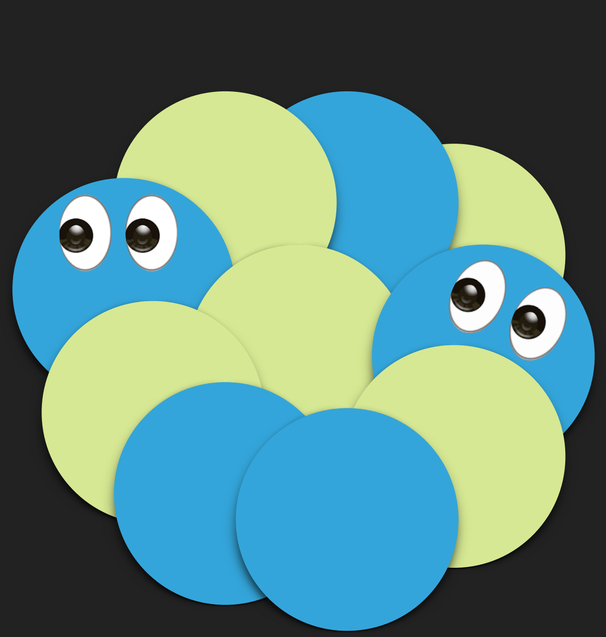

(A, Z)

$\longrightarrow$

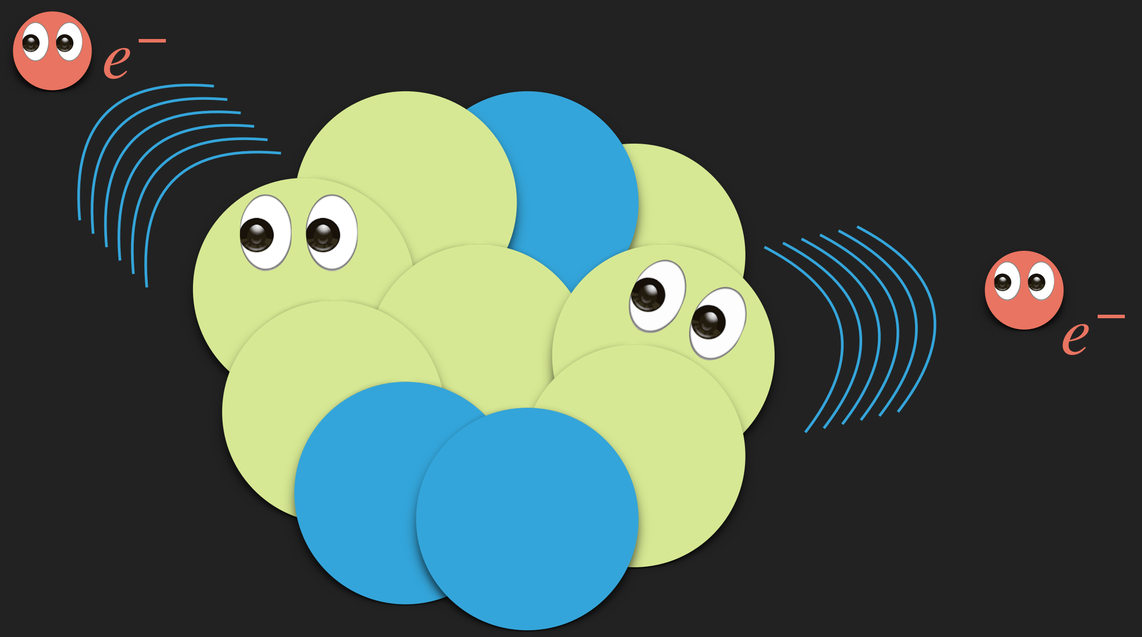

$(A, Z+2) + 2e^-$

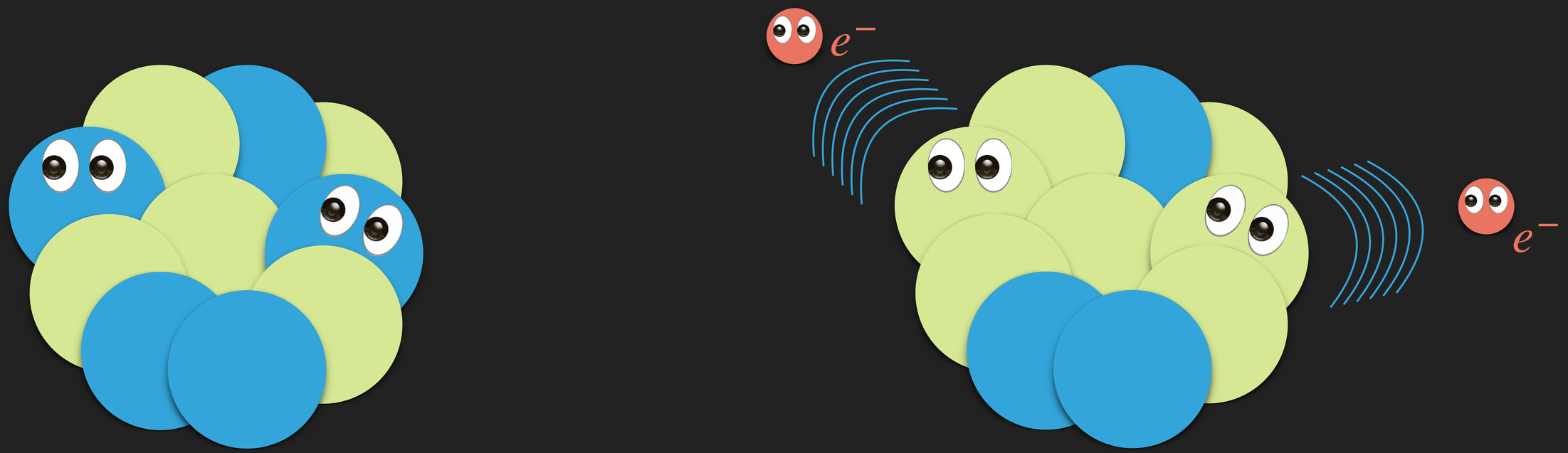

$$(A, Z) \longrightarrow (A, Z+2) + 2e^-$$

- Not yet observed
- Forbidden in the Standard Model : $|\Delta L| = 2$
- Majorana nature of ν

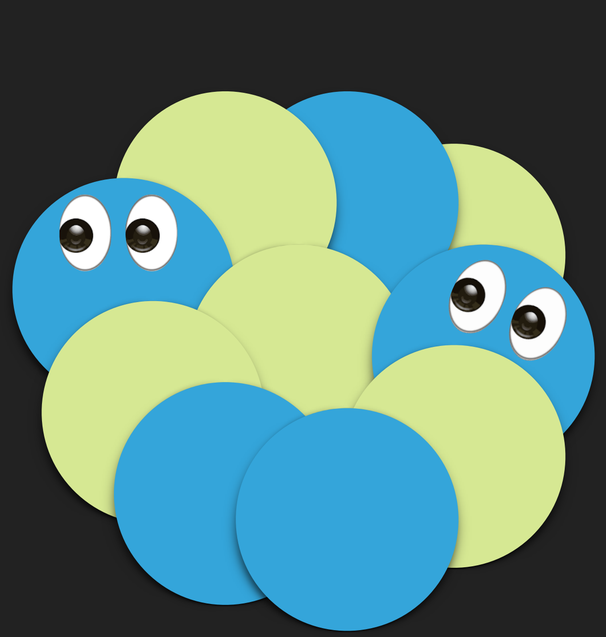

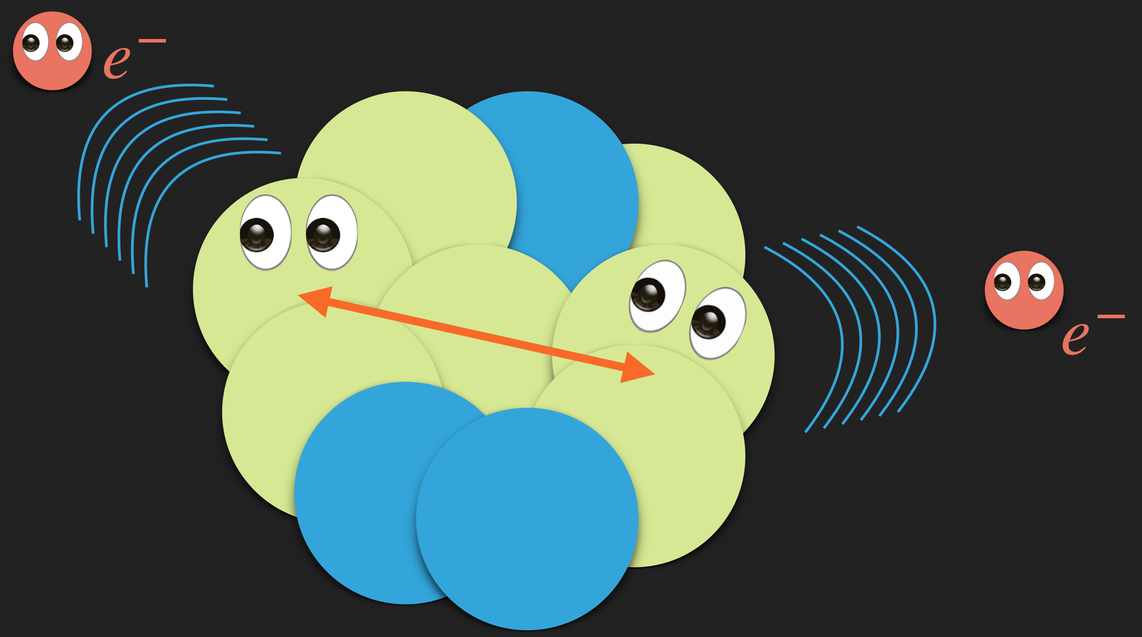

$$\Gamma_\alpha(m_{\beta\beta}, M_{\alpha i}) = G_{0\nu} \times (g_A^2 |M_{\alpha i}|)^2 \times \varepsilon_{\mathrm{BSM}}$$

Phase Space Factor (PSF) (kinematic)

Nuclear Matrix Element (NME)

Lepton number violation (LNV)

If $0\nu\beta\beta$ mediated by the exchange of a light-Majorana ν :

Effective Majorana mass

$$\left|\sum_j U_{ej}^2 m_j\right| = m_{\beta\beta}$$

$$\Gamma_\alpha(m_{\beta\beta}, M_{\alpha i}) = G_{0\nu} \times (g_A^2 |M_{\alpha i}|)^2 \times m_{\beta\beta}$$

- Does not require any extension of the SM in terms of particle content
- Directly connected to neutrino masses and neutrino mass ordering

If $0\nu\beta\beta$ mediated by the exchange of a light-Majorana ν :

Effective Majorana mass

$$\left|\sum_j U_{ej}^2 m_j\right| = m_{\beta\beta}$$

$$\Gamma_\alpha(m_{\beta\beta}, M_{\alpha i}) = G_{0\nu} \times (g_A^2 |M_{\alpha i}|)^2 \times m_{\beta\beta}$$

LOWER LIMITS ON THE DECAYING ISOTOPE HALF-LIFE ...

^{136}Xe

Loaded liquid scintillator

KAMLAND-ZEN

KamLAND-Zen (2024)

$T^{0\nu}_{1/2} > 3.8 \times 10^{26}$ yr

Xe-TPC

EXO-200

EXO-200 (2019)

$T^{0\nu}_{1/2} > 0.35 \times 10^{26}$ yr

^{76}Ge

High-purity Ge-detectors

GERDA

GERDA (2020)

$T^{0\nu}_{1/2} > 1.8 \times 10^{26}$ yr

MAJORANA

Majorana (2022)

$T^{0\nu}_{1/2} > 0.83 \times 10^{26}$ yr

^{130}Te

Cryogenic calorimeter

CUORE

CUORE (2022)

$T^{0\nu}_{1/2} > 0.22 \times 10^{26}$ yr

... TRANSLATED INTO UPPER BOUNDS ON $m_{\beta\beta}$

^{136}Xe

Loaded liquid scintillator

KAMLAND-ZEN

KamLAND-Zen (2024)

$m_{\beta\beta} < 28 - 122$ meV

Xe-TPC

EXO-200

EXO-200 (2019)

$m_{\beta\beta} < 93 - 286$ meV

^{76}Ge

High-purity Ge-detectors

GERDA

GERDA (2020)

$m_{\beta\beta} < 79 - 180$ meV

MAJORANA

Majorana (2022)

$m_{\beta\beta} < 113 - 269$ meV

^{130}Te

Cryogenic calorimeter

CUORE

CUORE (2022)

$m_{\beta\beta} < 90 - 305$ meV

... TRANSLATED INTO UPPER BOUNDS ON $m_{\beta\beta}$

^{136}Xe

Loaded liquid scintillator

KAMLAND-ZEN

KamLAND-Zen (2024)

$m_{\beta\beta} < 28 - 122$ meV

Xe-TPC

EXO-200

EXO-200 (2019)

$m_{\beta\beta} < 93 - 286$ meV

^{76}Ge

High-purity Ge-detectors

GERDA

GERDA (2020)

$m_{\beta\beta} < 79 - 180$ meV

MAJORANA

Majorana (2022)

$m_{\beta\beta} < 113 - 269$ meV

^{130}Te

Cryogenic calorimeter

CUORE

CUORE (2022)

$m_{\beta\beta} < 90 - 305$ meV

$T^{0\nu}_{1/2} > 10^{28}$ yr

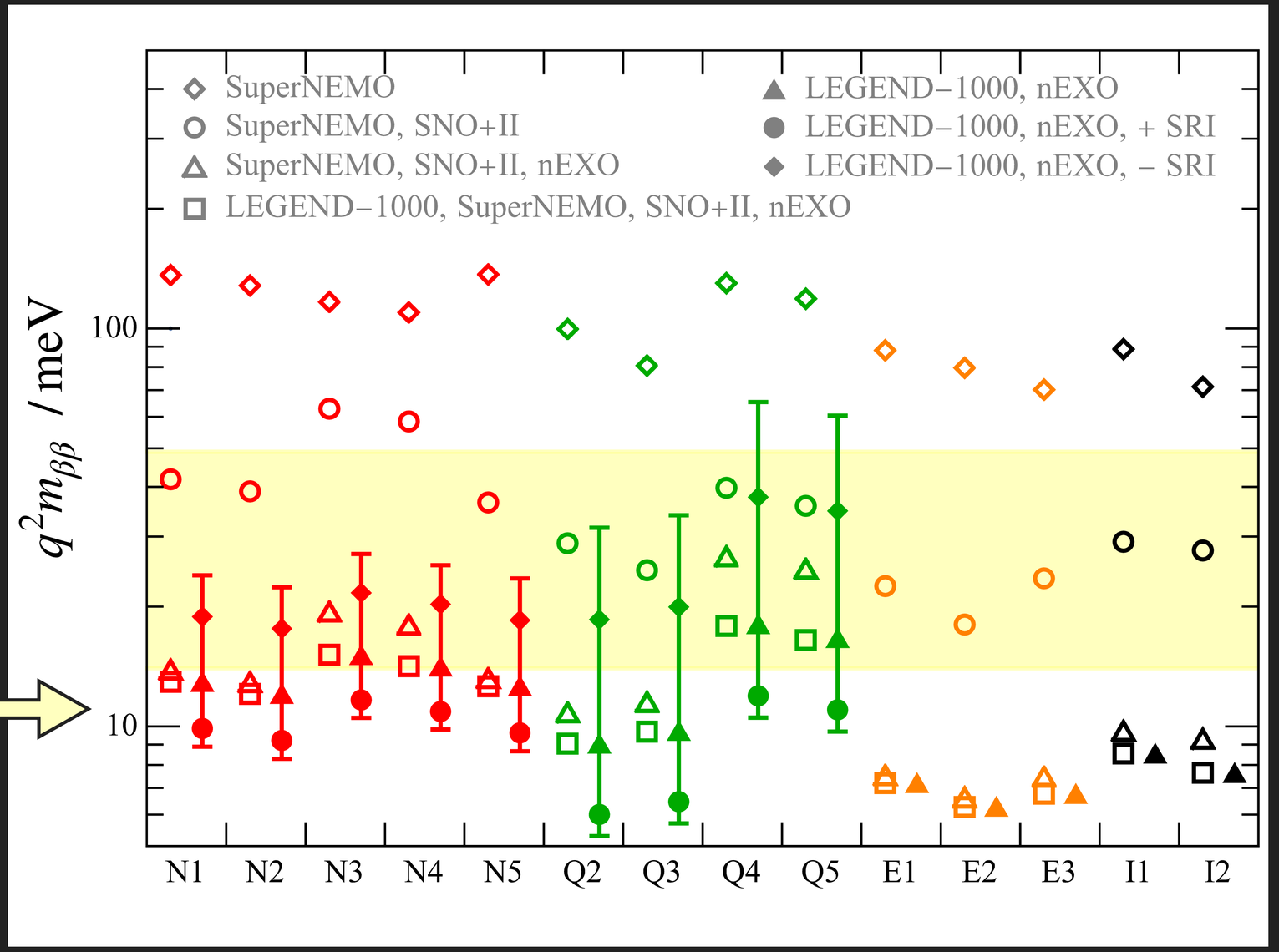

F.Pompa, T.Schwetz, J-Y.Zhu(JHEP 06 (2023) 104)

$$\Gamma_\alpha(m_{\beta\beta}, M_{\alpha i}) = G_{0\nu} \times (g_{\mathrm{A}}^2 |M_{\alpha i}|)^2 \times$$

Mass mechanism ($d = 5$)

$$\Gamma_{\alpha}(m_{\beta\beta}, M_{\alpha i}) = G_{0\nu} \times (g_{\mathrm{A}}^2 |M_{\alpha i}|)^2 \times \begin{cases} \text{Leptoquark Models } (d > 5) \\ \text{Mass mechanism } (d = 5) \\ \text{Left-Right Symmetric Models } (d > 5) \end{cases}$$

$$\Gamma_{\alpha}(m_{\beta\beta}, M_{\alpha i}) = G_{0\nu} \times (g_{\mathrm{A}}^2 |M_{\alpha i}|)^2 \times \begin{cases} \text{Leptoquark Models } (d > 5) \\ \text{Mass mechanism } (d = 5) \\ \text{Left-Right Symmetric Models } (d > 5) \end{cases}$$

Assuming a future $0\nu\beta\beta$ signal detection, would it be possible to discriminate the dominant LNV mechanism driving the decay?

$$\Gamma_{\alpha}(m_{\beta\beta}, M_{\alpha i}) = G_{0\nu} \times (g_{\mathrm{A}}^2 \mid M_{\alpha i} \mid)^2 \times \begin{cases} \text{Leptoquark Models } (d > 5) \\ \text{Mass mechanism } (d = 5) \\ \text{Left-Right Symmetric Models } (d > 5) \end{cases}$$

Kinematic observables!

Assuming a future $0\nu\beta\beta$ signal detection, would it be possible to discriminate the dominant LNV mechanism driving the decay?

$$\Gamma_\alpha(m_{\beta\beta}, M_{\alpha i}) = G_{0\nu} \times (g_A^2 |M_{\alpha i}|)^2 \times \langle m_{\beta\beta} \rangle$$

$$\Gamma_\alpha(m_{\beta\beta}, M_{\alpha i}) = G_{0\nu} \times (g_A^2 |M_{\alpha i}|)^2 \times \begin{cases} \mathrm{VL}(6) \\ \langle m_{\beta\beta} \rangle \\ \mathrm{VR}(6) \end{cases}$$

$$\Gamma_\alpha(m_{\beta\beta}, M_{\alpha i}) = G_{0\nu} \times (g_A^2 |M_{\alpha i}|)^2 \times \begin{cases} \text{VL(6)} \\ \langle m_{\beta\beta} \rangle \\ \text{VR(6)} \end{cases}$$

KINEMATIC OBSERVABLES :

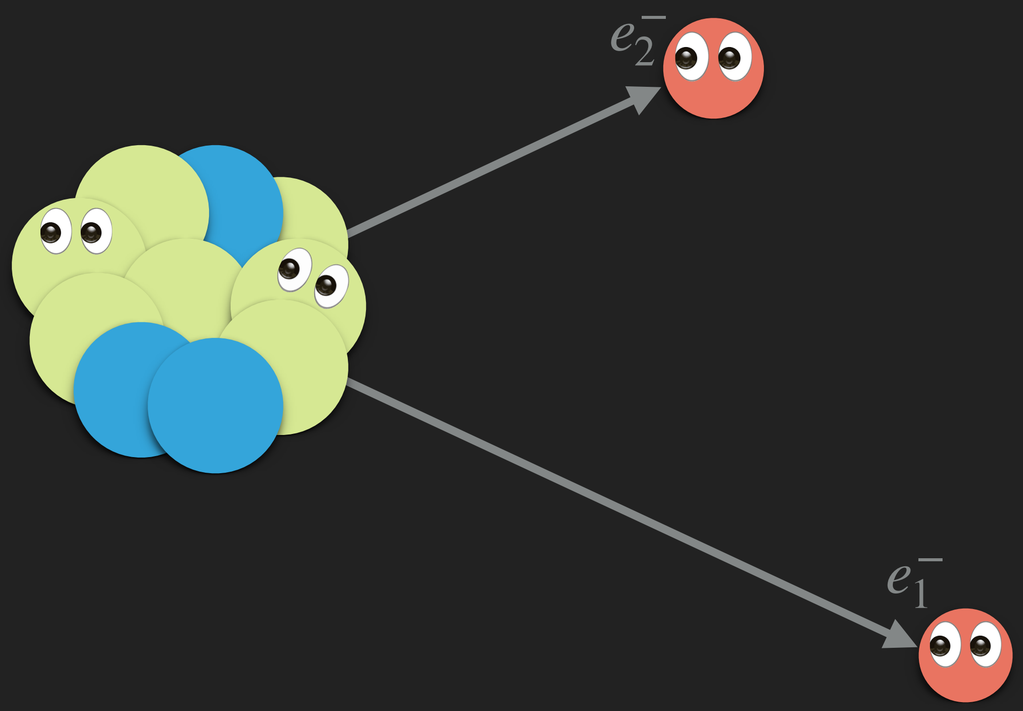

$$\Gamma_\alpha(m_{\beta\beta}, M_{\alpha i}) = G_{0\nu} \times (g_A^2 |M_{\alpha i}|)^2 \times \begin{cases} \text{VL(6)} \\ \langle m_{\beta\beta} \rangle \\ \text{VR(6)} \end{cases}$$

KINEMATIC OBSERVABLES :

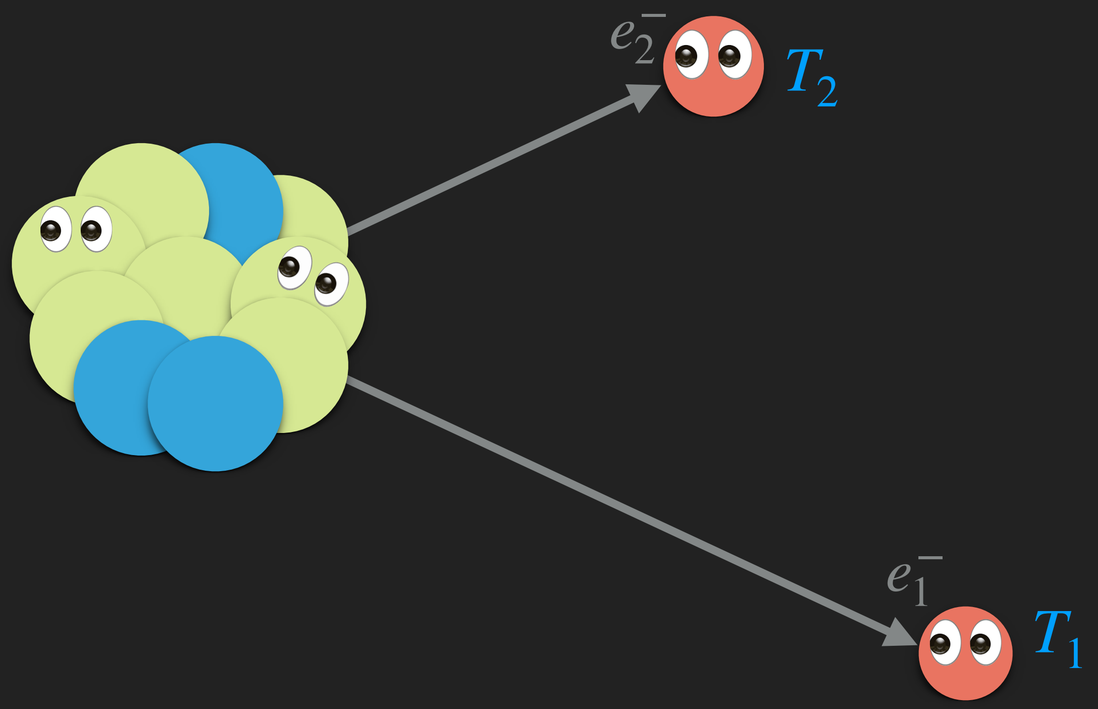

Single-electron kinetic energy distribution

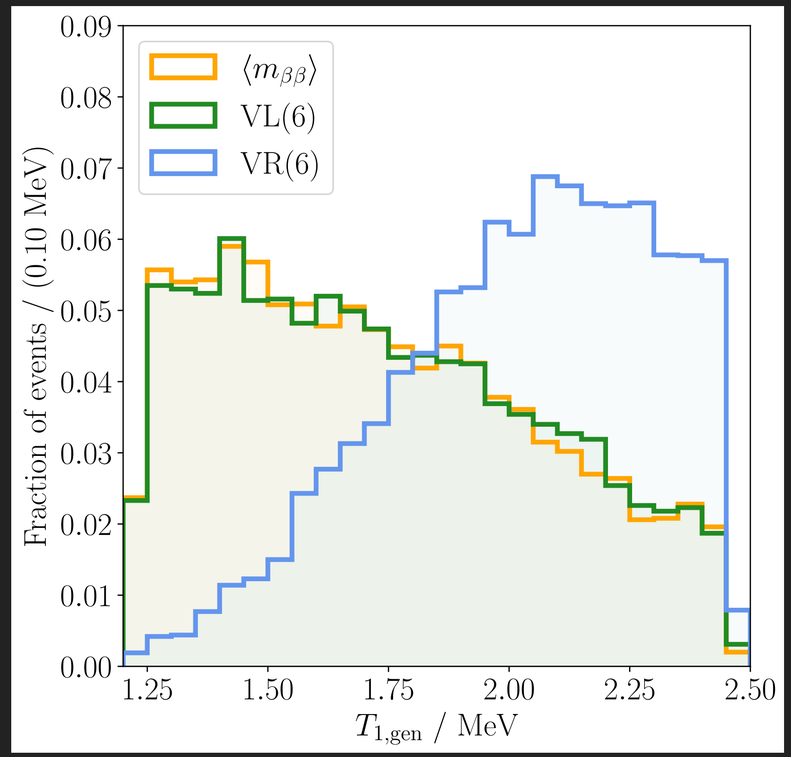

$$\Gamma_\alpha(m_{\beta\beta}, M_{\alpha i}) = G_{0\nu} \times (g_A^2 |M_{\alpha i}|)^2 \times \begin{cases} \text{VL(6)} \\ \langle m_{\beta\beta} \rangle \\ \text{VR(6)} \end{cases}$$

KINEMATIC OBSERVABLES :

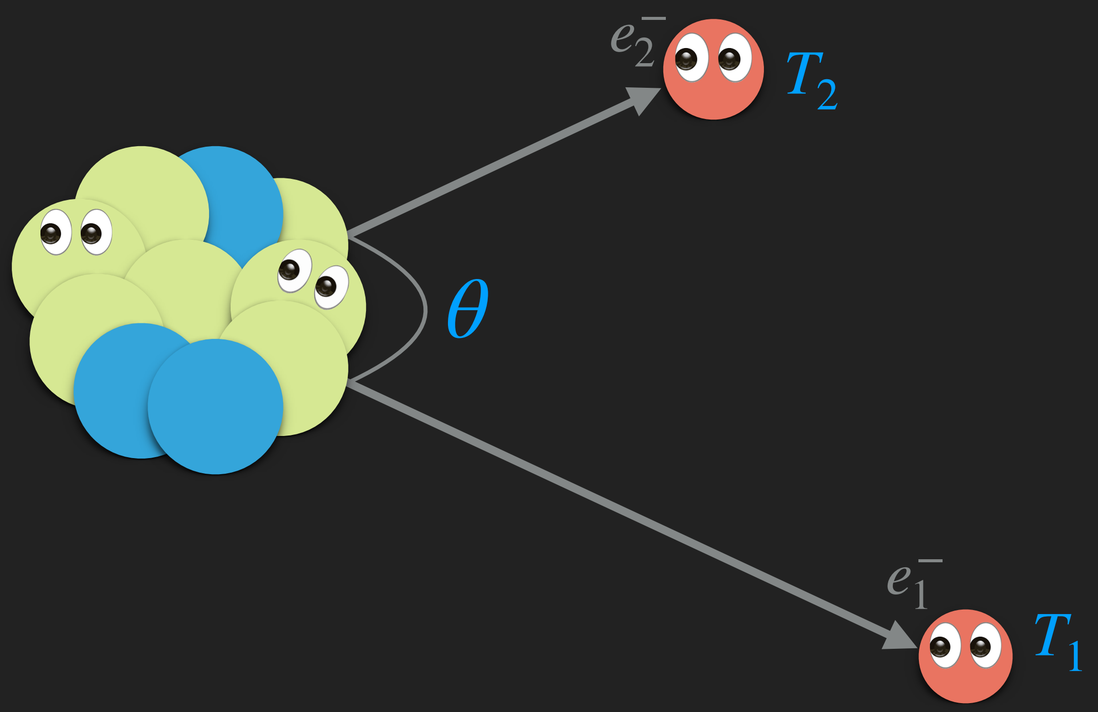

Opening angle distribution

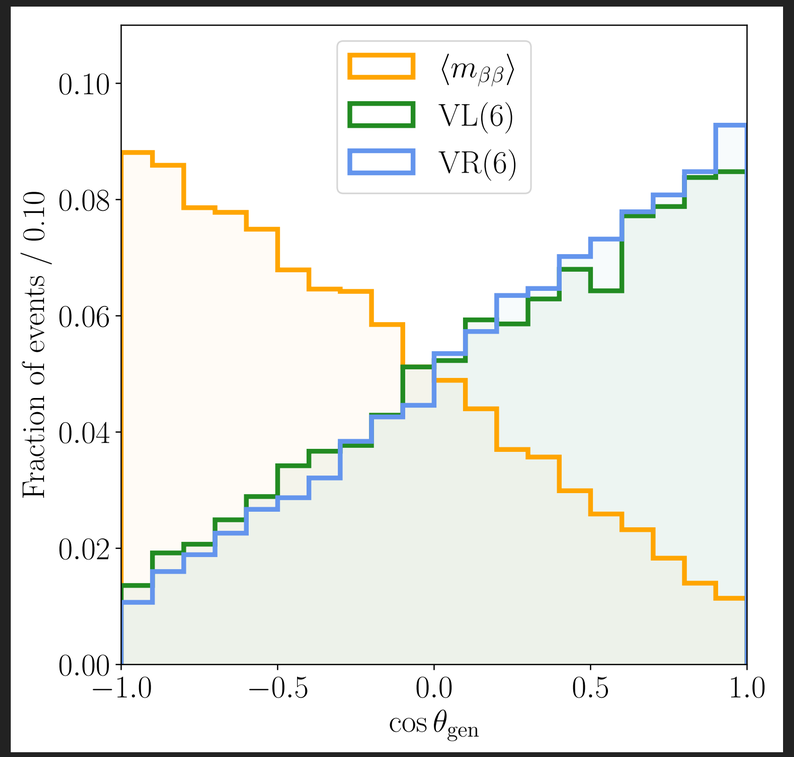

$$\Gamma_\alpha(m_{\beta\beta}, M_{\alpha i}) = G_{0\nu} \times (g_A^2 |M_{\alpha i}|)^2 \times \begin{cases} \mathrm{VL}(6) \\ \langle m_{\beta\beta} \rangle \\ \mathrm{VR}(6) \end{cases}$$

O.Scholer, J.de Vries, L.Gráf (JHEP 08 (2023) 043)

Single-electron kinetic energy distribution

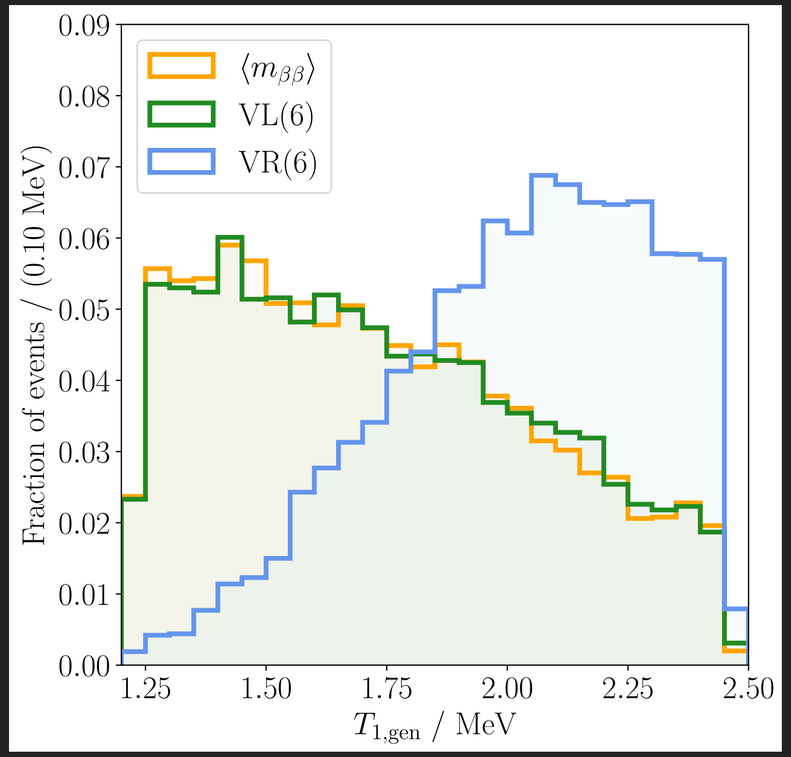

Opening angle distribution

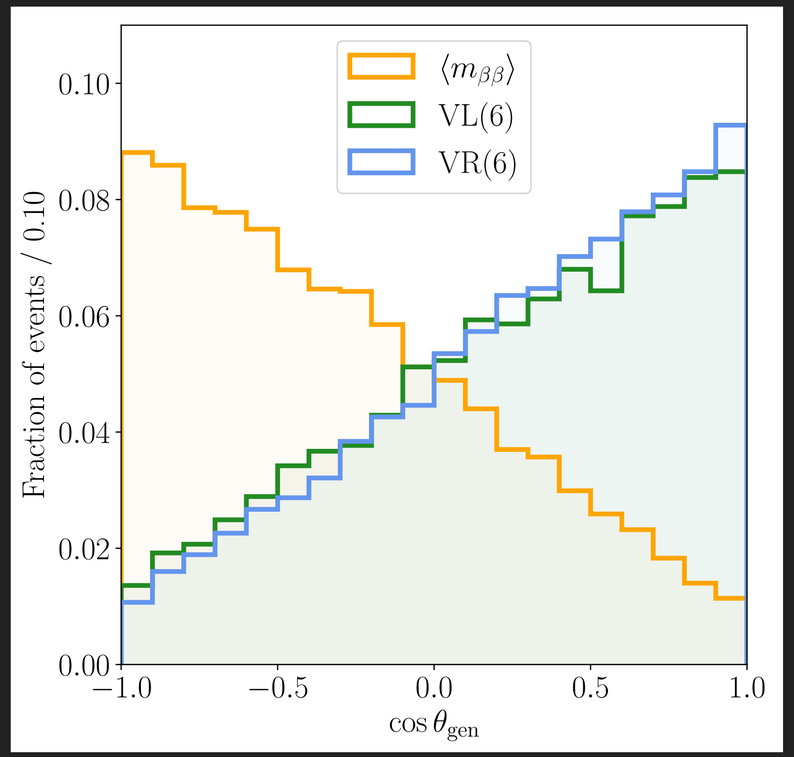

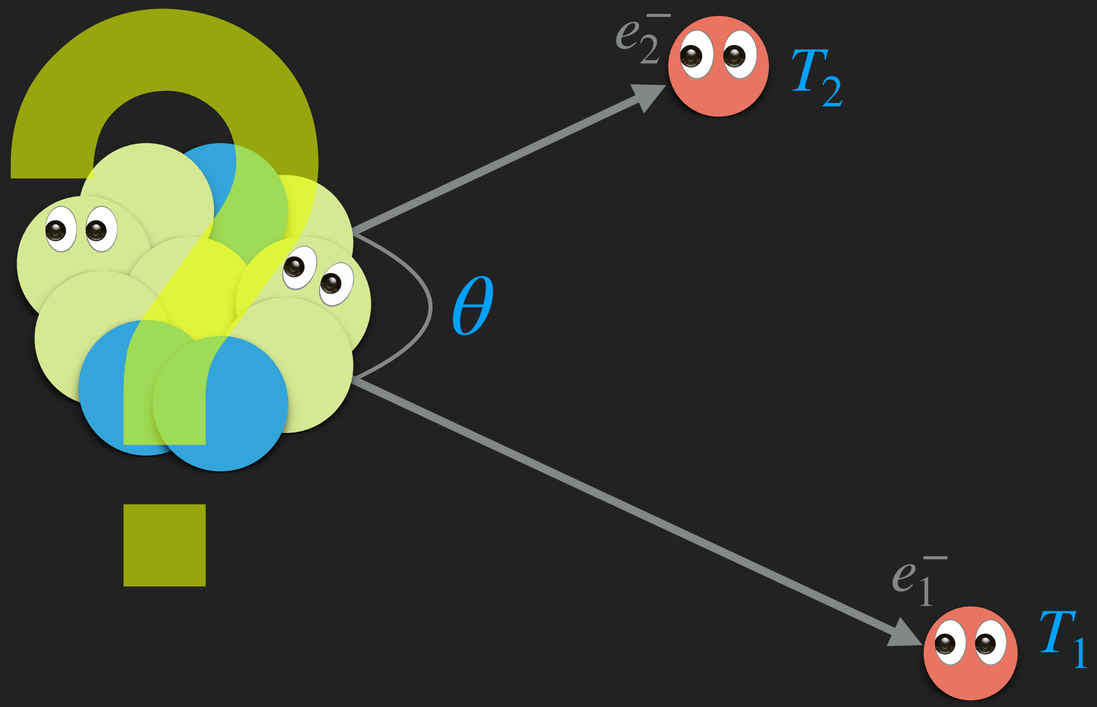
e_2^-
T_2
θ
e_1^-
T_1

Topological studies of $0\nu\beta\beta$ signal require

- precise localization of the decay vertex
- good electron track reconstruction

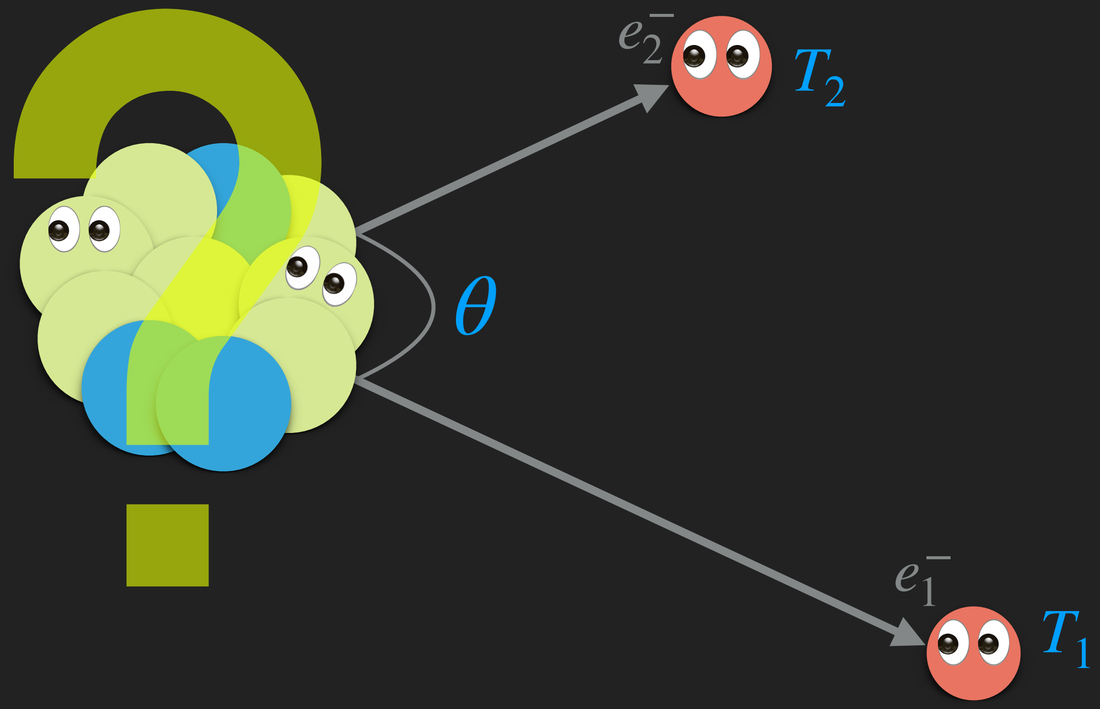

BARIUM-TAGGING FOR XENON-GAS TPC DETECTORS

$$^{136}Xe \longrightarrow {}^{136}Ba^{++} + 2e^{-}$$

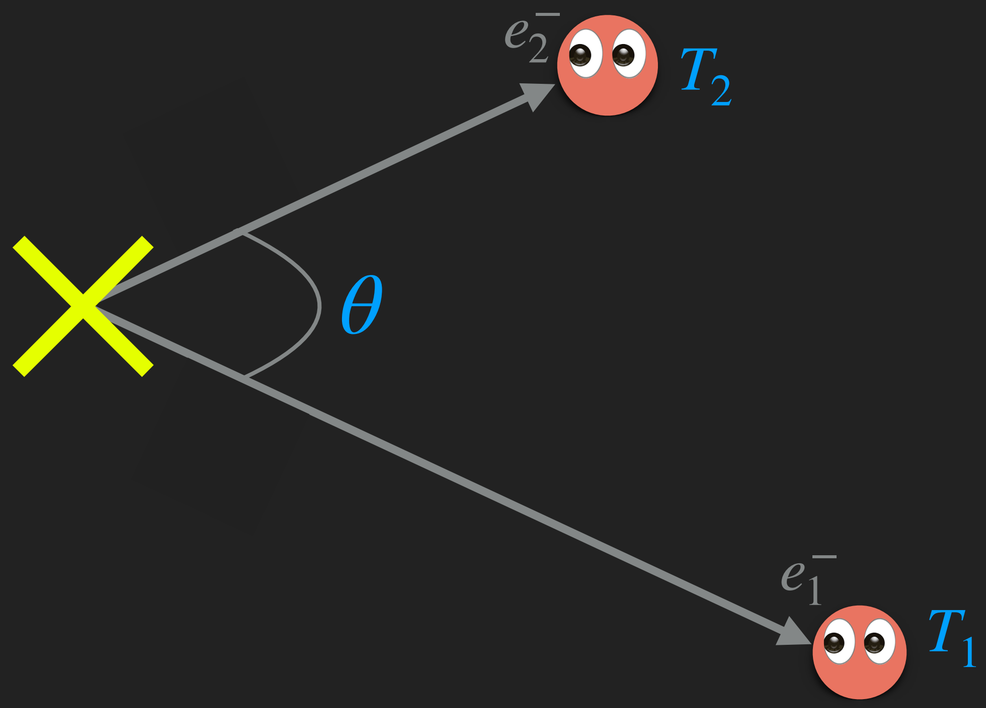

Topological studies of $0\nu\beta\beta$ signal require

- precise localization of the decay vertex
- good electron track reconstruction

Single-Molecule Fluorescence Imaging techniques

NEXT Collaboration (Phys.Rev.Lett.120)

Currently under investigation and planned to be employed in the future upgrade of the NEXT detector


$\vec{E}_{\text{drift}}$
$\vec{E}_{\text{extr}}$
Energy plane : S1
Cathode
Anode
Electro-Luminescence region : S2
Tracking plane
Pressurized vessel


$\vec{E}_{\text{drift}}$
$\vec{E}_{\text{extr}}$
Energy plane : S1
Cathode
Anode
Electro-Luminescence region : S2
Tracking plane
e^-
e^-
e^-
e^-
e^-
Pressurized vessel


$\vec{E}_{\text{drift}}$
$\vec{E}_{\text{extr}}$
Energy plane : S1
Cathode
Anode
Electro-Luminescence region : S2
Tracking plane
e^-
e^-
e^-
e^-
e^-
Pressurized vessel

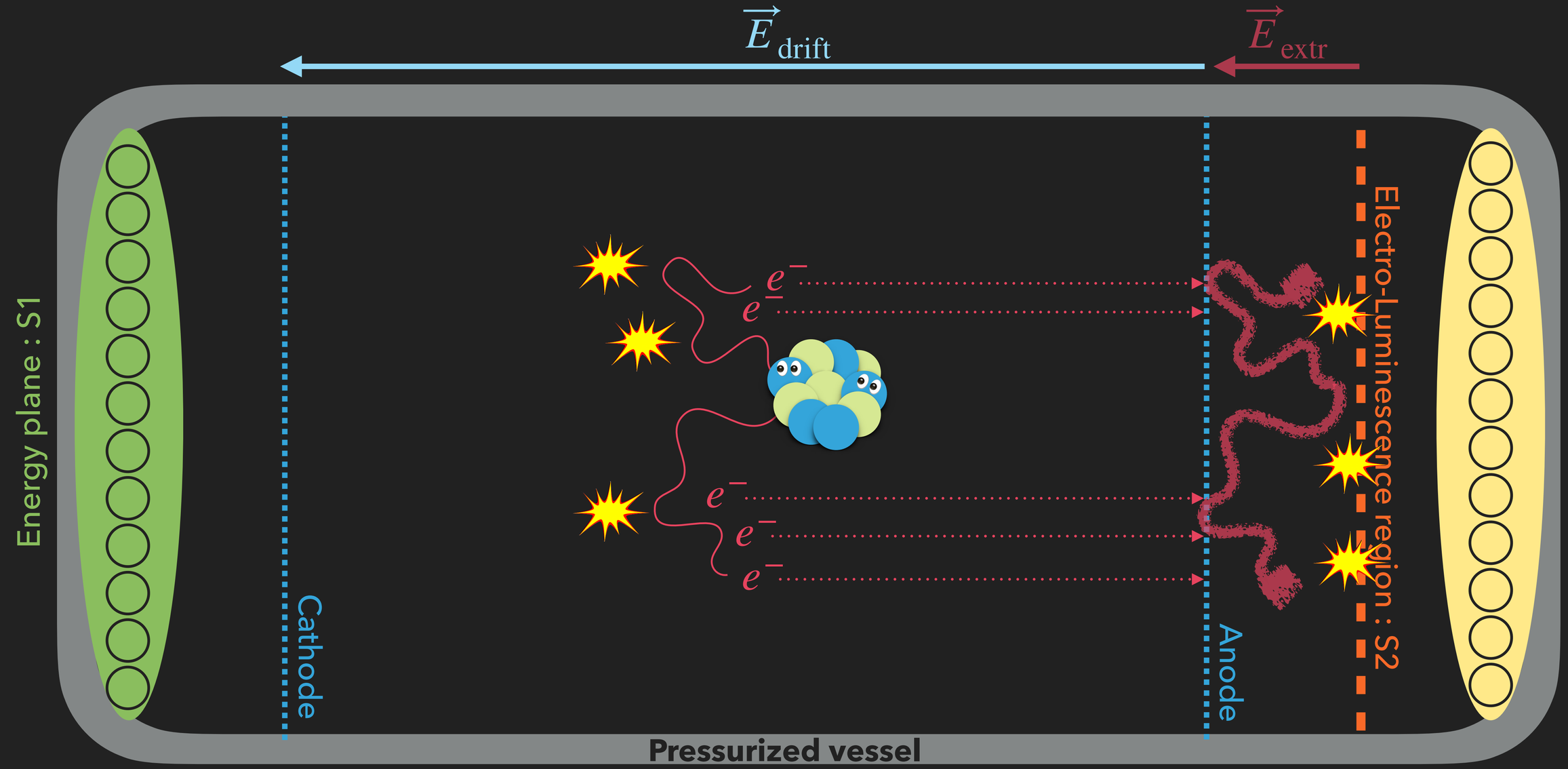
$\vec{E}_{\text{drift}}$
$\vec{E}_{\text{extr}}$
Energy plane : S1
Cathode
Anode
Electro-Luminescence region : S2
Tracking plane
Pressurized vessel
e^-
e^-
e^-
e^-
e^-

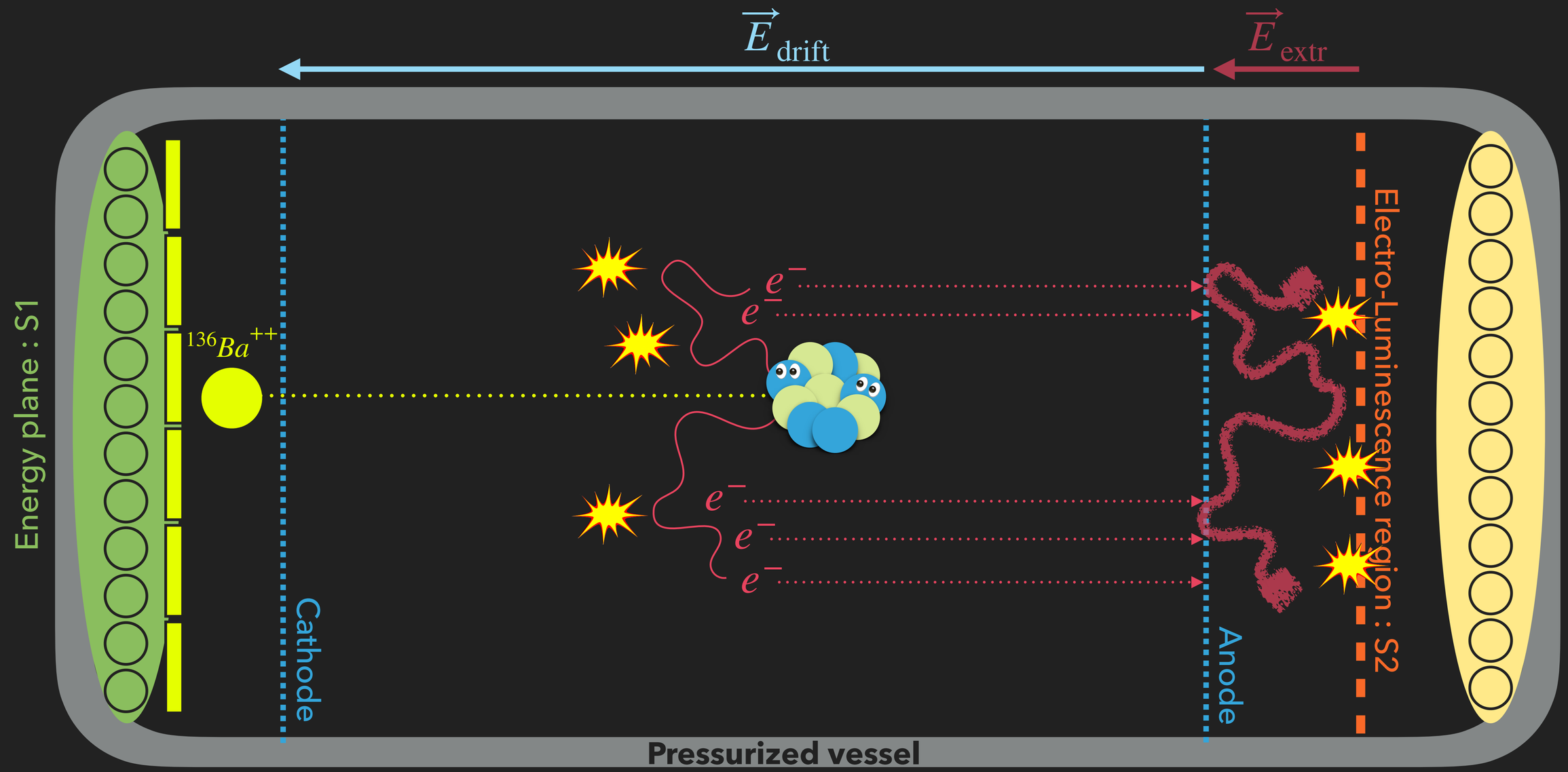
$\vec{E}_{\text{drift}}$
$\vec{E}_{\text{extr}}$
Energy plane : S1
$^{136}Ba^{++}$
e^-
e^-
e^-
e^-
e^-
Cathode
Anode
Electro-Luminescence region : S2
Tracking plane
Pressurized vessel

IN A XENON-GAS TPC DETECTOR WITH VERTEX-TAGGING CAPABILITY

IN A XENON-GAS TPC DETECTOR WITH VERTEX-TAGGING CAPABILITY

GEN

Generation (νDoBe)

Theoretical prediction for electron kinetic energy and opening angle distributions of different LNV contributions.

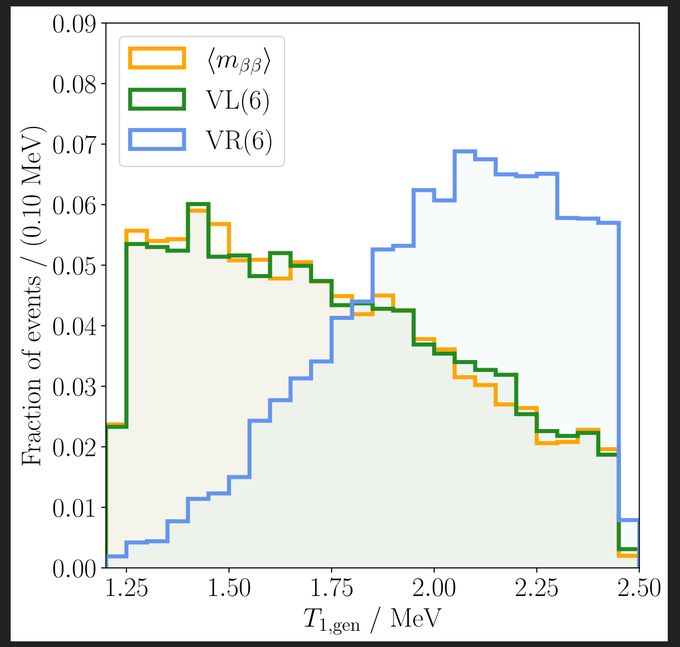

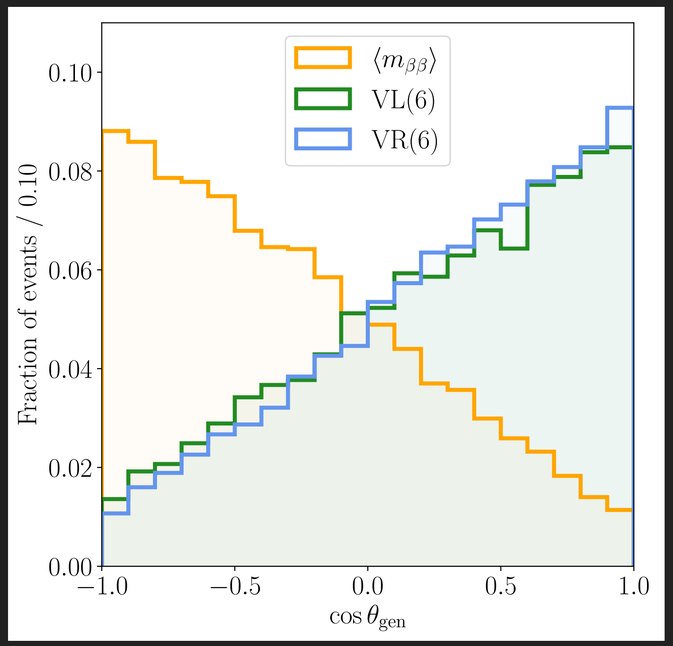

IN A XENON-GAS TPC DETECTOR WITH VERTEX-TAGGING CAPABILITY

GEN

Generation (νDoBe)

Theoretical prediction for electron kinetic energy and opening angle distributions of different LNV contributions.

TRUE

Propagation in the detector (GEANT4-nexus)

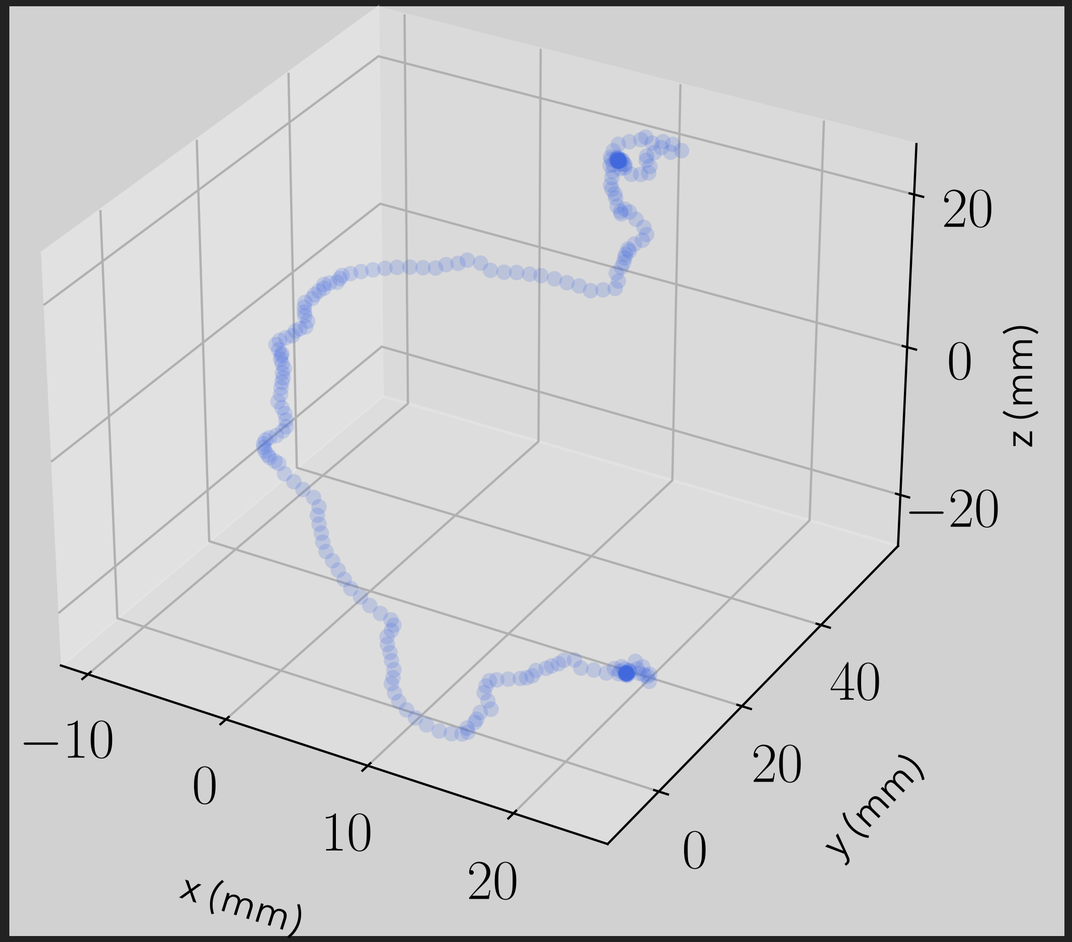

IN A XENON-GAS TPC DETECTOR WITH VERTEX-TAGGING CAPABILITY

GEN

Generation (νDoBe)

Theoretical prediction for electron kinetic energy and opening angle distributions of different LNV contributions.

TRUE

Propagation in the detector (GEANT4-nexus)

Barium-tagging for vertex localization.

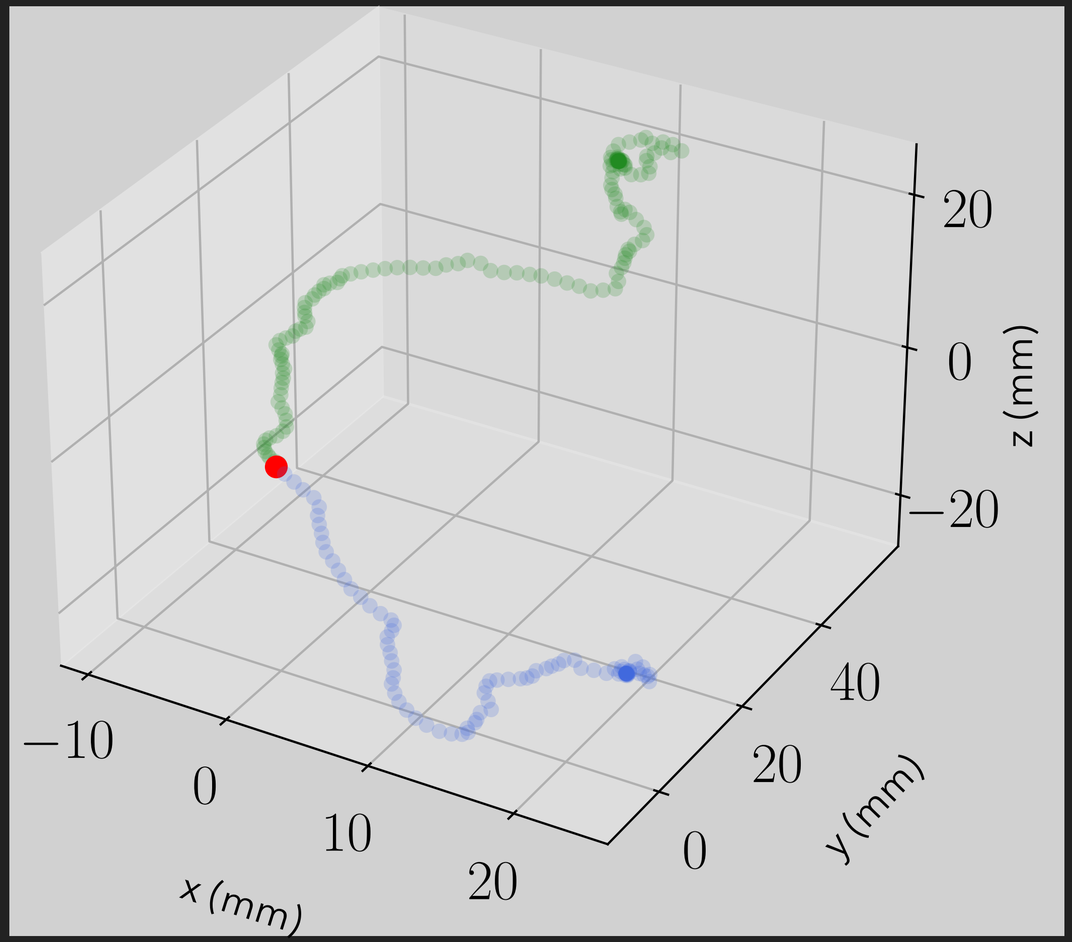

IN A XENON-GAS TPC DETECTOR WITH VERTEX-TAGGING CAPABILITY

GEN

Generation (νDoBe)

Theoretical prediction for electron kinetic energy and opening angle distributions of different LNV contributions.

TRUE

Propagation in the detector (GEANT4-nexus)

Barium-tagging for vertex localization.

RECO

Reconstruction

Algorithm to sort GEANT4 hits based on the minimum-distance criterium.

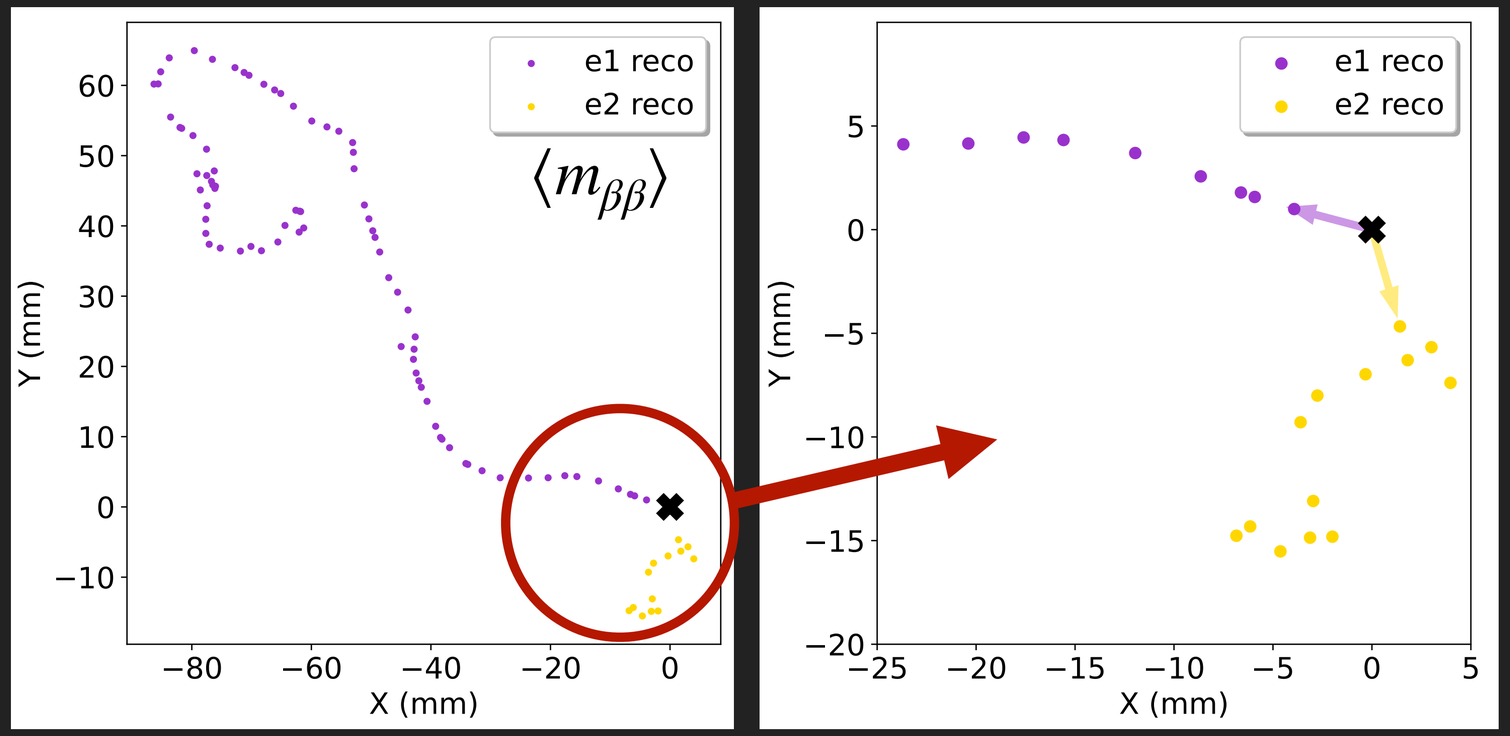

F.Pompa & the NEXT Collaboration (ArXiv:2502.10198)

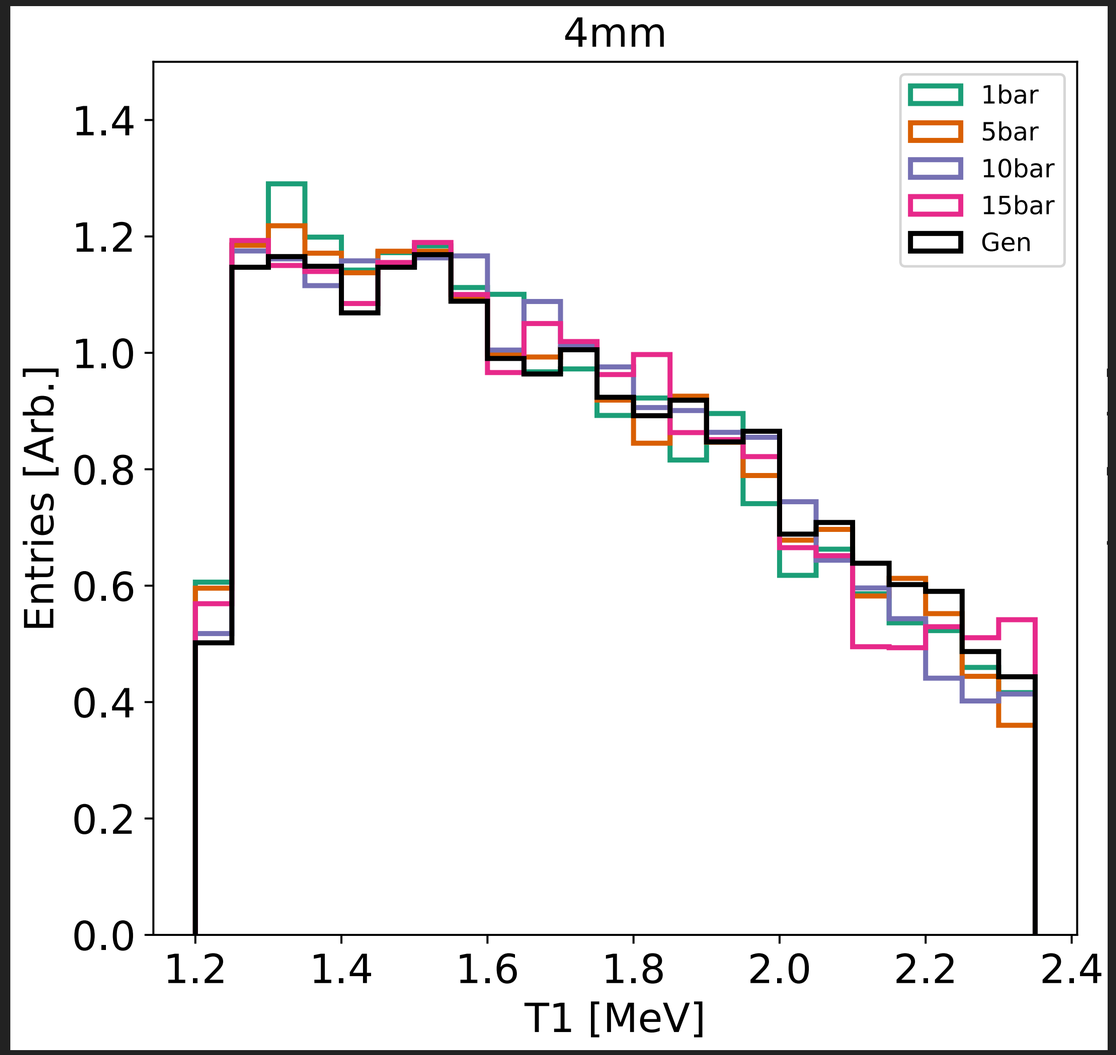

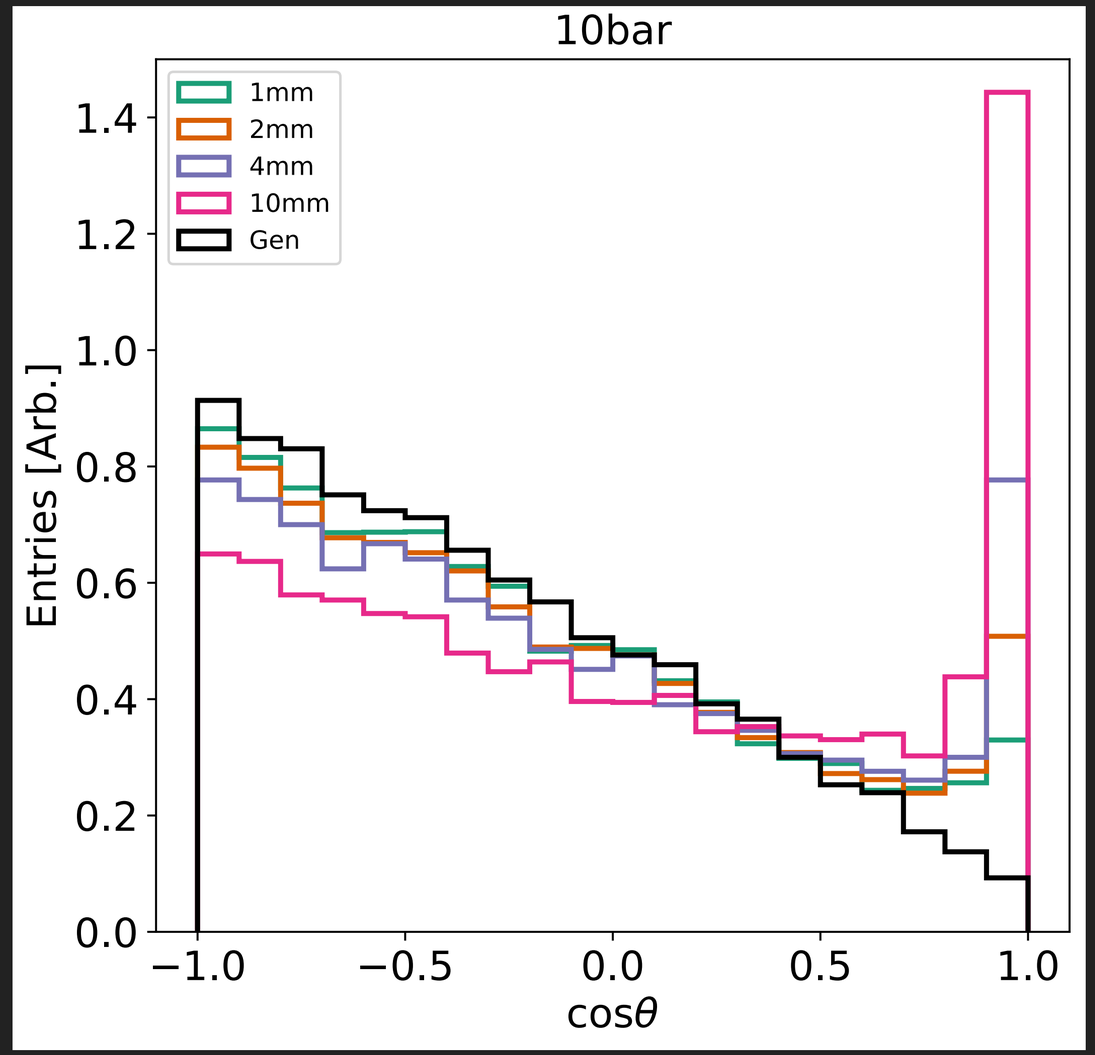

Discrimination performances: combined sensitivity

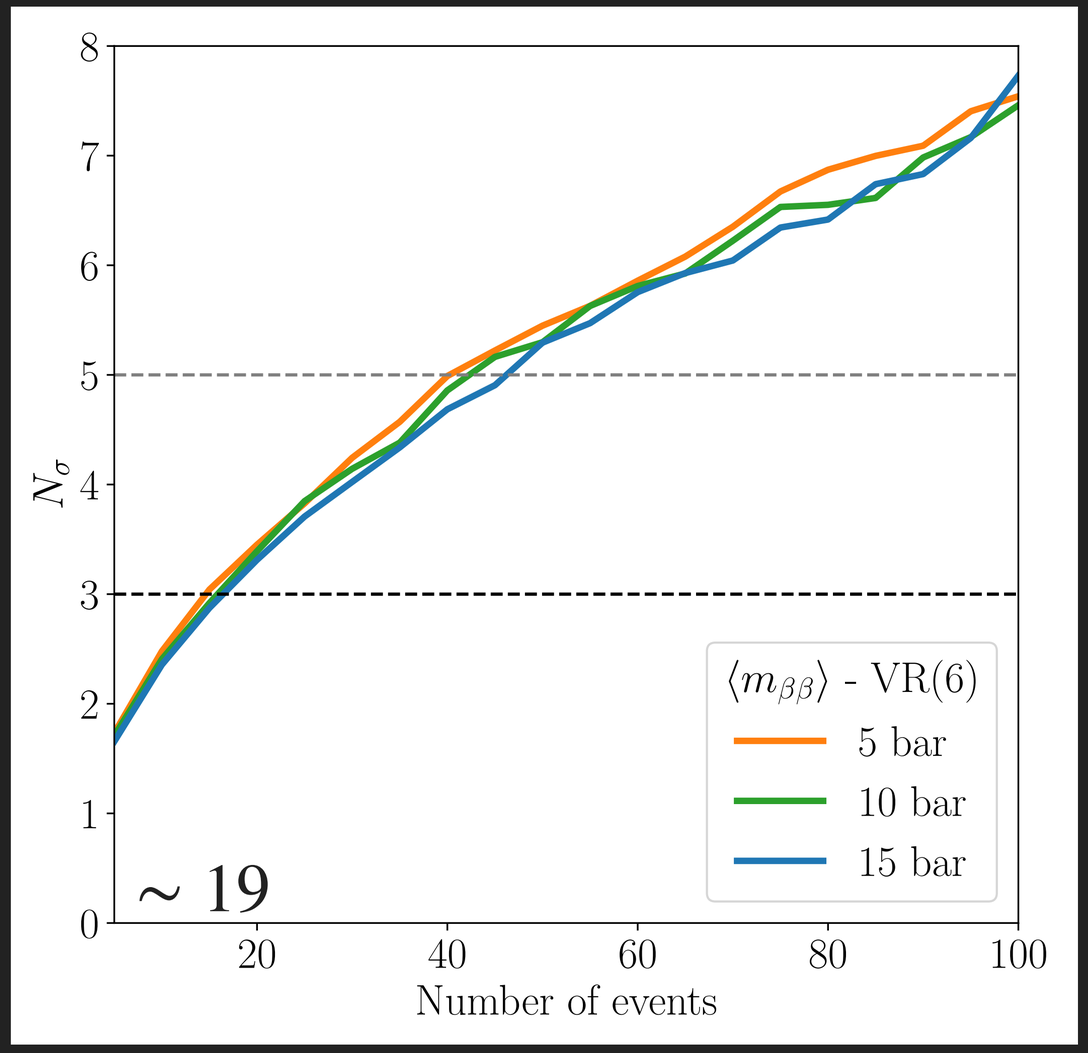

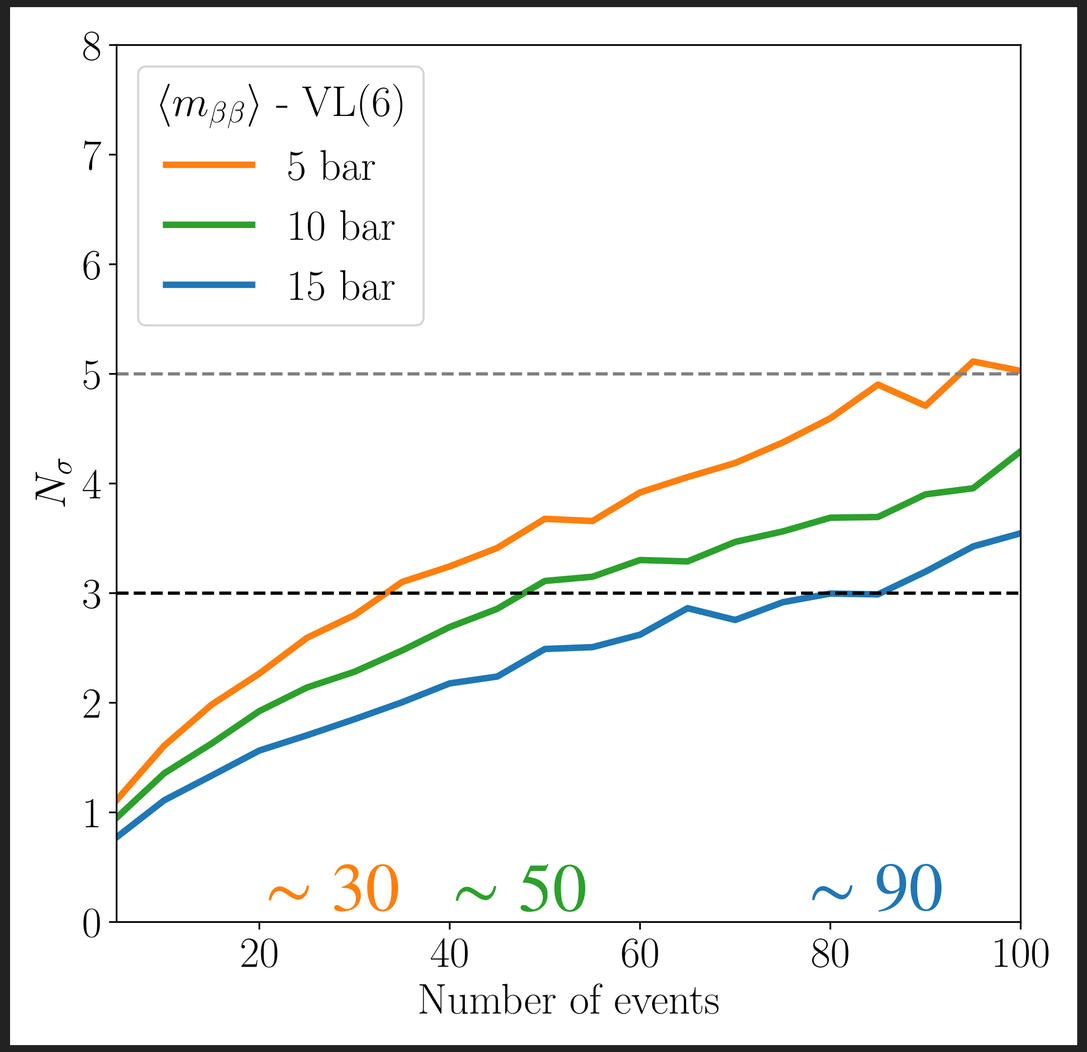

Discrimination performances: combined sensitivity

Assuming a future $0\nu\beta\beta$ signal detection, would it be possible to discriminate the dominant LNV mechanism driving the decay?

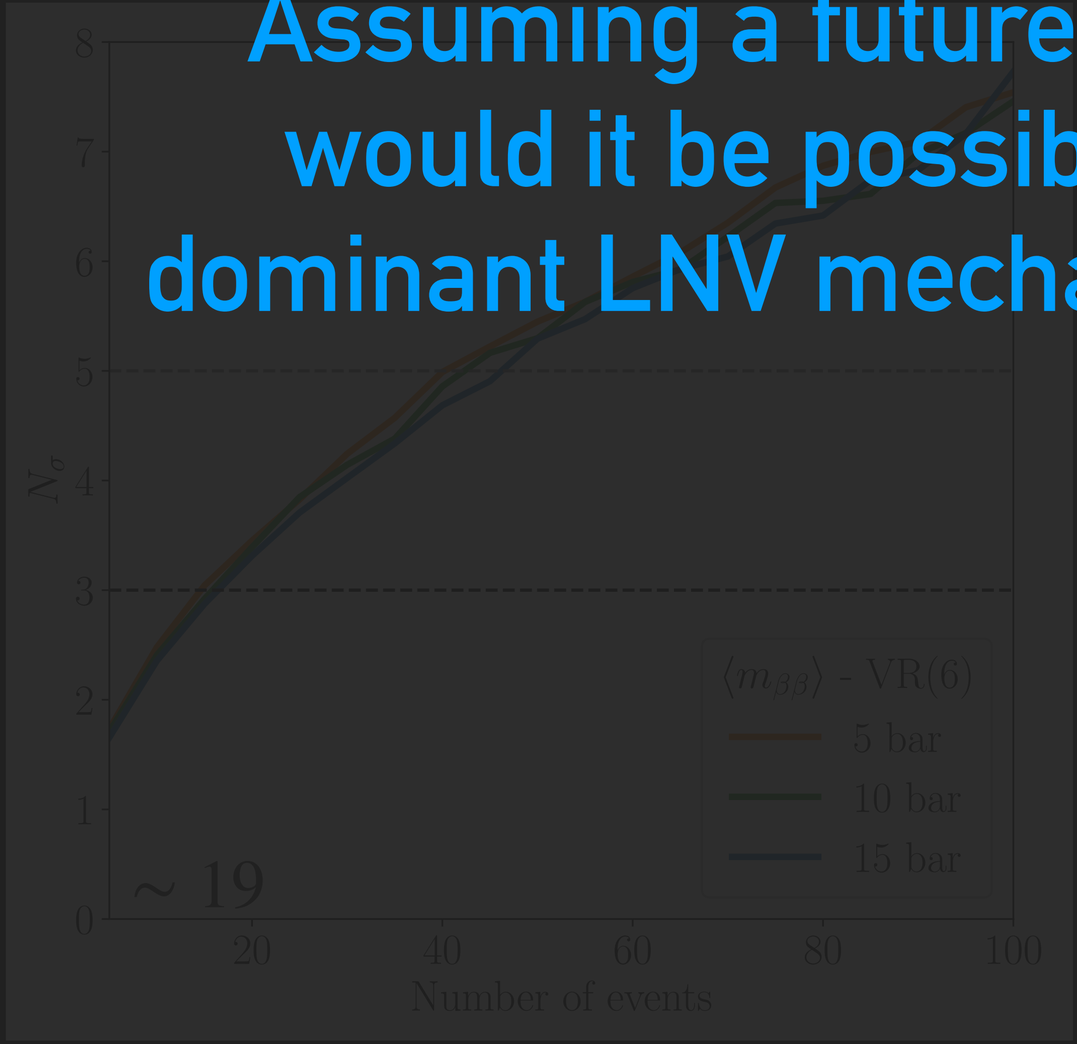

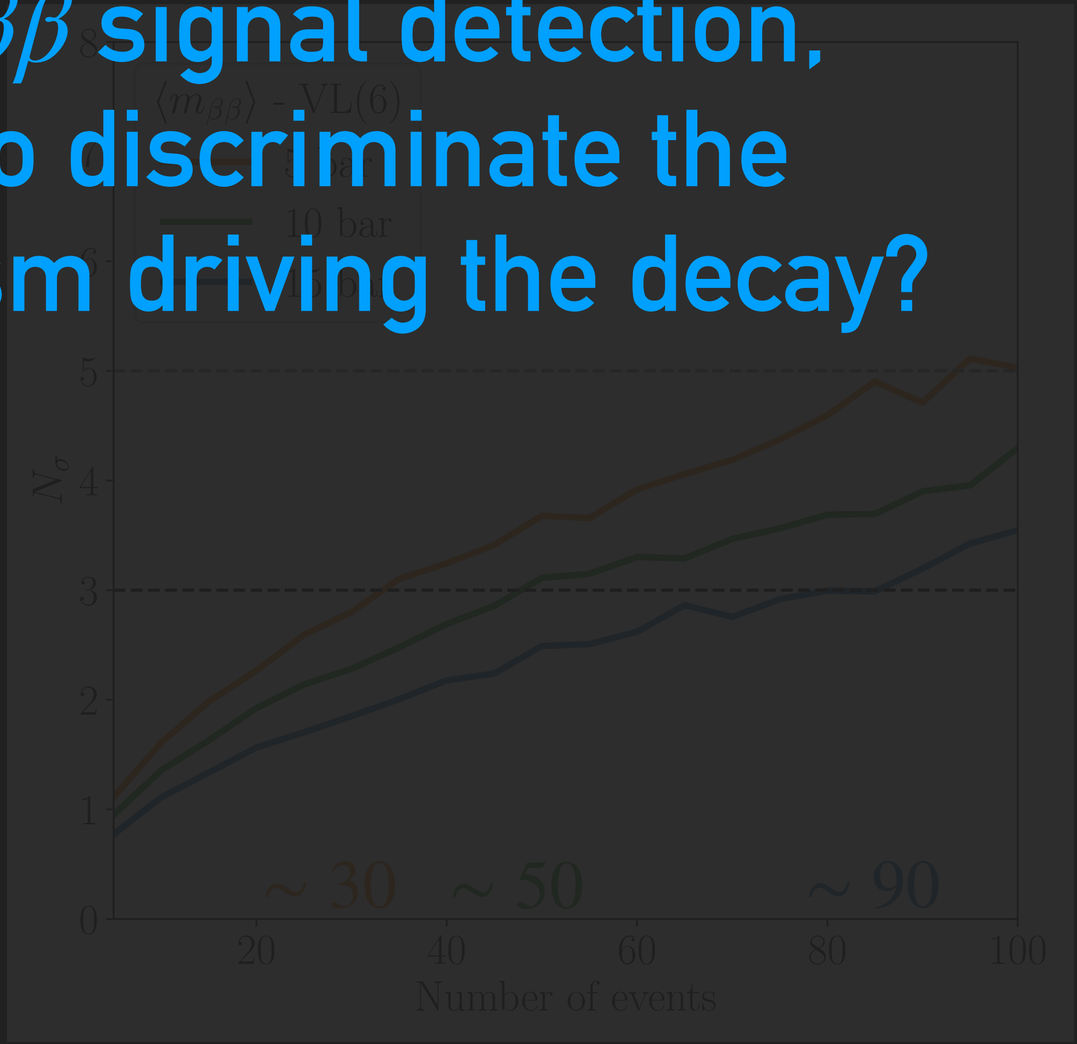

Discrimination performances: combined sensitivity

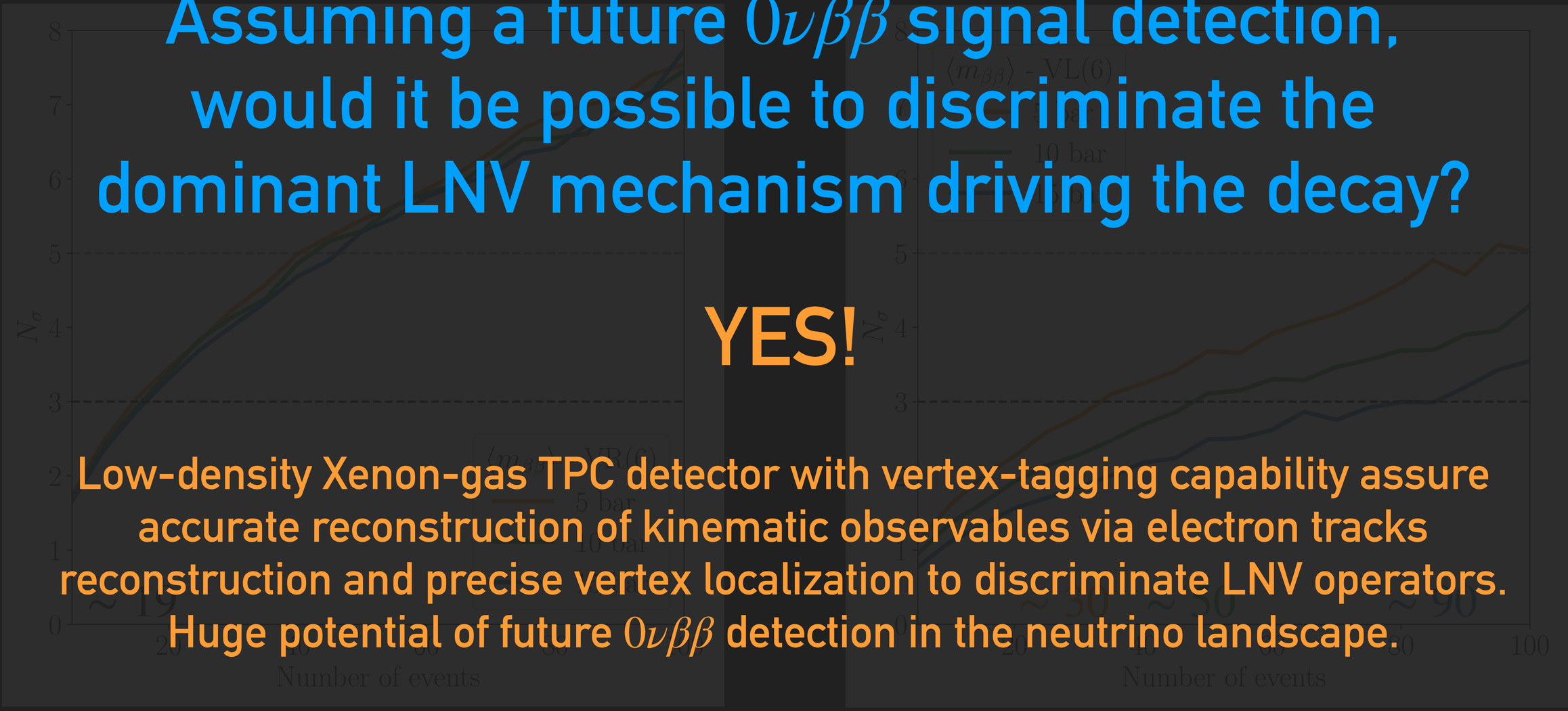

Assuming a future $0\nu\beta\beta$ signal detection, would it be possible to discriminate the dominant LNV mechanism driving the decay?

YES!

Low-density Xenon-gas TPC detector with vertex-tagging capability assure accurate reconstruction of kinematic observables via electron tracks reconstruction and precise vertex localization to discriminate LNV operators.
Huge potential of future $0\nu\beta\beta$ detection in the neutrino landscape.

The lack of knowledge on the underlying dominant LNV contribution to $0\nu\beta\beta$, and the complexity in describing the nuclear structure of the initial and final nuclei, constitute the most limiting theoretical factors in $0\nu\beta\beta$ searches.

The lack of knowledge on the underlying dominant LNV contribution to $0\nu\beta\beta$, and the complexity in describing the nuclear structure of the initial and final nuclei, constitute the most limiting theoretical factors in $0\nu\beta\beta$ searches.

Improved treatment of nuclear effects to improve accuracy of phenomenological predictions

- Effective Field Theory approaches to provide a systematic framework to include and evaluate the effects of nuclear forces and quantifying their uncertainties.

Additional efforts to reduce theoretical uncertainties from nuclear physics calculations (ab-initio methods)

- Rigorous theoretical approach to describe nuclear structure and reactions, without relying on empirical inputs.
- Computationally expensive and difficult to apply these universally across all nuclei.

BACKUP

Nuclear Models and NME with light-Majorana neutrinos

Long-range contribution to the decay rate induced by the exchange of light-Majorana ν

$$M_{\alpha i} = M_{\alpha i}^{\text{long}}$$

$$(r \sim 1.2\, A^{1/3}\ \text{fm})$$

- 4 many-body nuclear models
- Calculations performed by different groups by assuming $g_{\text{A}}^{\text{bare}} = 1.27$
- Data not available for all the isotopes
- Variation in $M_{\alpha i}^{\text{long}}$ of a factor ~ 3

M.Agostini et all. - Rev.Mod.Phys. 95 (2023) 2, 025002

$i \downarrow$	$\alpha \rightarrow$	^{76}Ge	^{82}Se	^{100}Mo	^{130}Te	^{136}Xe
Nuclear Shell Model	N1	2.89	2.73	-	2.76	2.28
	N2	3.07	2.90	-	2.96	2.45
	N3	3.37	3.19	-	1.79	1.63
	N4	3.57	3.39	-	1.93	1.76
	N5	2.66	2.72	-	3.16	2.39
Quasiparticle Random Phase Approximation	Q1	5.09	-	-	1.37	1.55
	Q2	5.26	3.73	3.90	4.00	2.91
	Q3	4.85	4.61	5.87	4.67	2.72
	Q4	3.12	2.86	-	2.90	1.11
	Q5	3.40	3.13	-	3.22	1.18
	Q6	-	-	-	4.05	3.38
Energy-Density Functional theory	E1	4.60	4.22	5.08	5.13	4.20
	E2	5.55	4.67	6.59	6.41	4.77
	E3	6.04	5.30	6.48	4.89	4.24
Interacting Boson Model	I1	5.14	4.19	3.84	3.96	3.25
	I2	6.34	5.21	5.08	4.15	3.40

Short-range NME for light-Majorana neutrinos

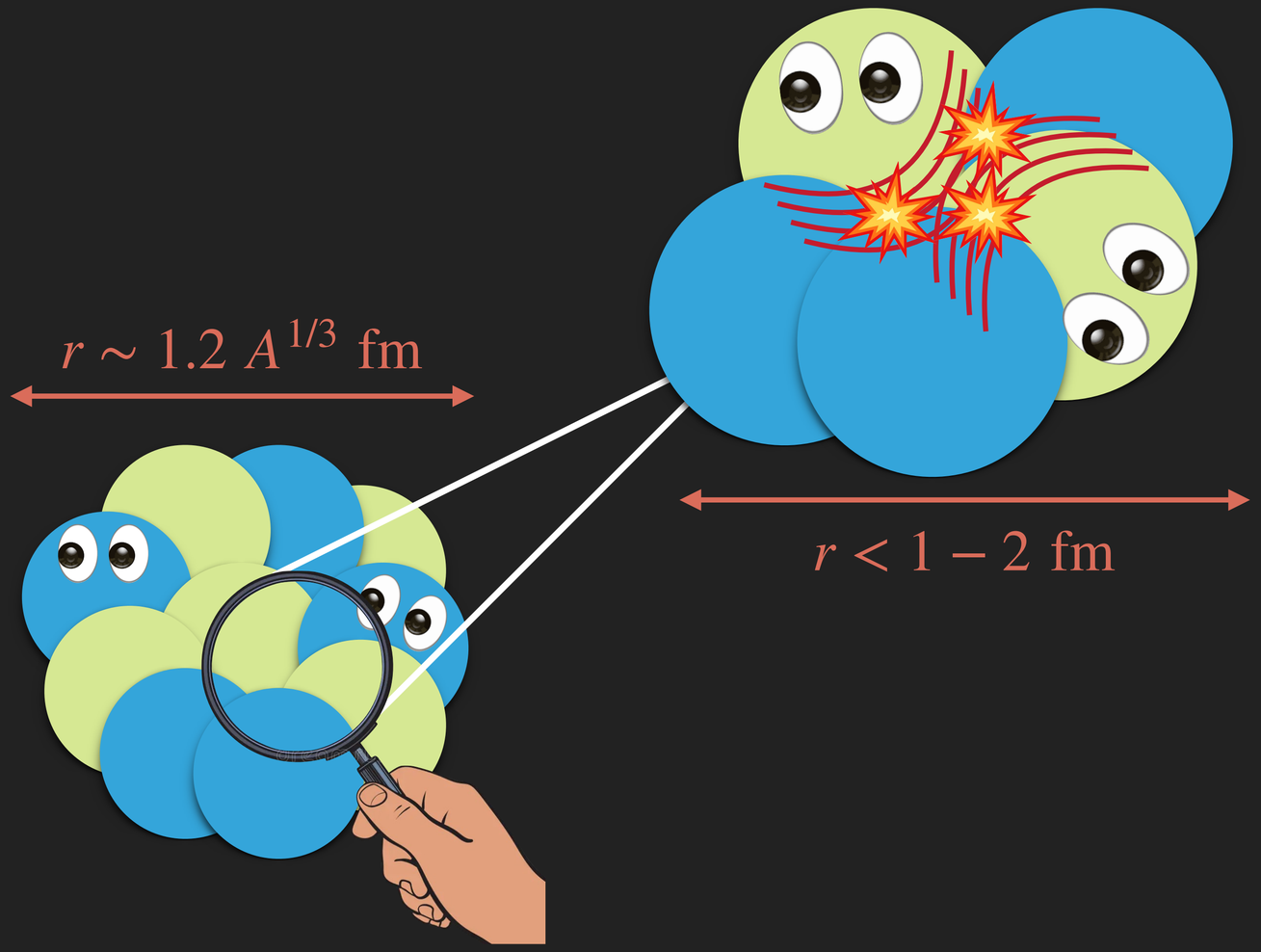

Correction accounting for the strong nuclear forces that become significant at close distances

$$M_{\alpha i} = M_{\alpha i}^{\text{long}} + M_{\alpha i}^{\text{short}} = M_{\alpha i}^{\text{long}}\left(1 + n_{\alpha i}\right)$$

Absolute value (%)

$i \rightarrow$ $\alpha \downarrow$	Nuclear Shell Model	Quasiparticle Random Phase Approximation
^{76}Ge	$15 \div 42$	$32 \div 73$
^{82}Se	$15 \div 42$	$30 \div 70$
^{100}Mo	-	$49 \div 108$
^{130}Te	$17 \div 47$	$34 \div 77$
^{136}Xe	$17 \div 47$	$30 \div 70$

Electron tracks within the gas

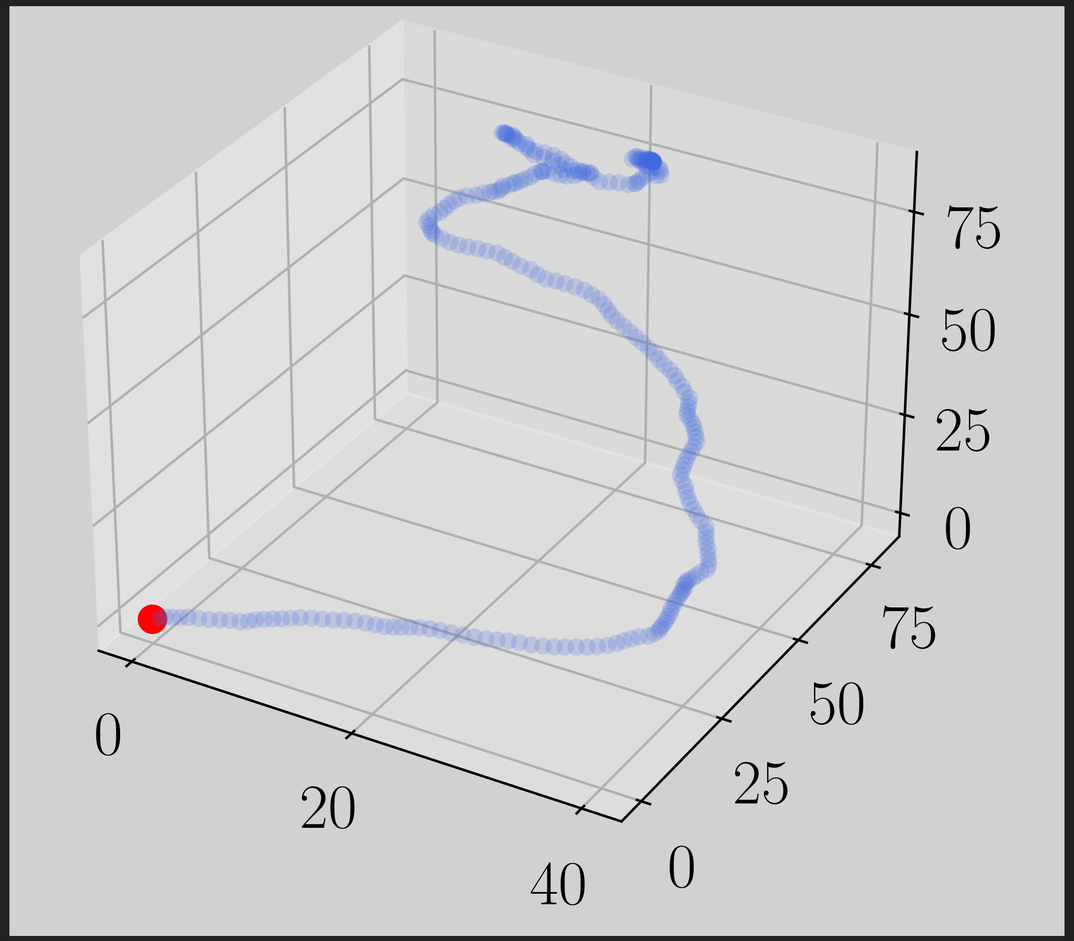

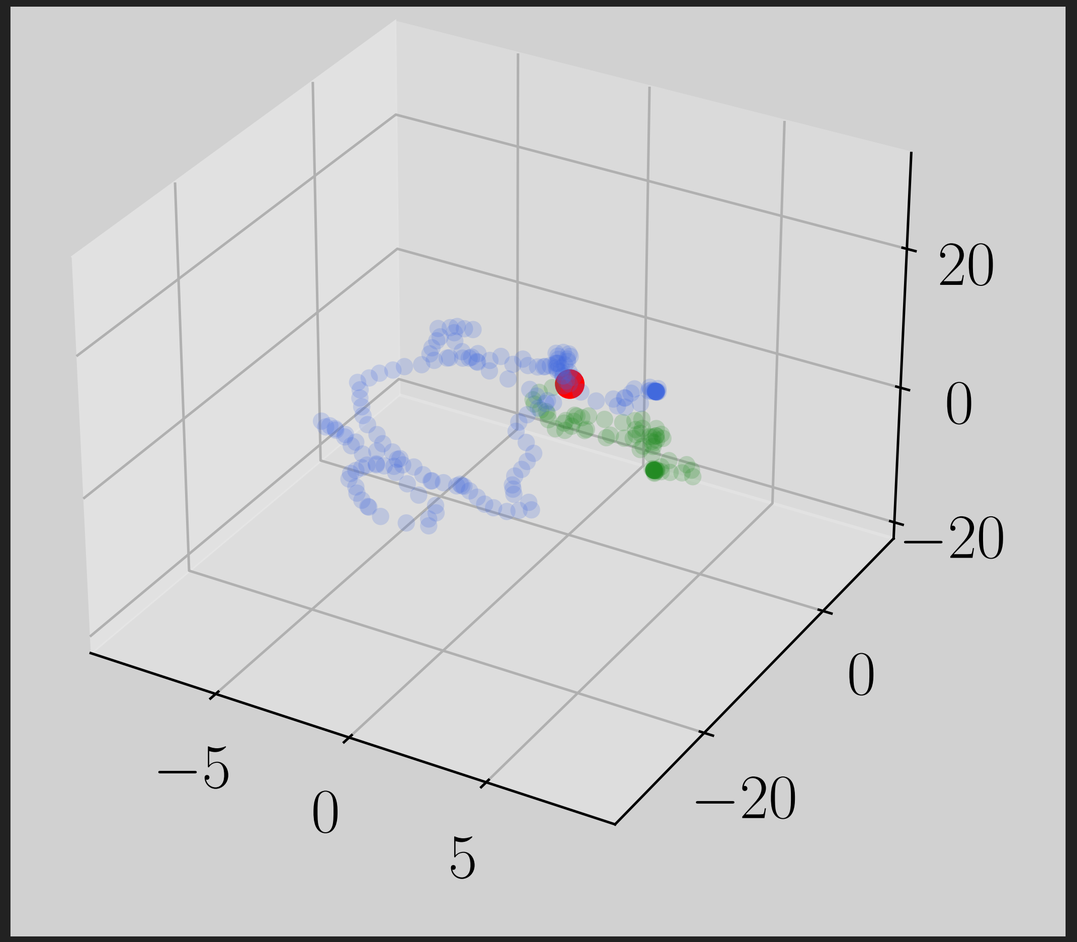

Experimental $0\nu\beta\beta$ techniques

High-purity Germanium detectors →

Excellent energy resolution (0.1% FWHM)
Source ≡ detector medium
Good signal-to-background discrimination power

Xenon Time-Projection Chambers →

Ionization charge + scintillation light (background rejection)
3D electron tracking
Self-shielding power (high atomic number and density)
Easy scalability to larger isotope masses

Loaded liquid scintillators →

Solar neutrino detectors loaded with $0\nu\beta\beta$ emitter
Already-proven ultra-low background environments
Limited energy resolution

Cryogenic calorimeters →

Very low temperatures and precise measurements of energy deposits
Source ≡ detector medium

Tracking calorimeters →

Multi-layers detection concept ($0\nu\beta\beta$ emitter - tracking chambers - calorimeter)
Kinematic observables reconstruction

Background sources for $0\nu\beta\beta$ experiments

Intrinsic $2\nu\beta\beta$ mode	Accurate measurement of the emitted electron energies
Cosmic ray induced processes	Constructing experiments in underground laboratories
Spallation induced by high-energy muon flux and leading to possible unstable nuclei activation	Detector shielding and delayed time-coincidence with the original muon event
Muon spallation in the rock surrounding that can generate penetrating high-energy neutrons	Embedding in the detector medium materials with high neutron capture cross section
Radioactivity of detector materials	Purification and selection of detector materials
Elastic Scattering or Charged-Current interactions of solar neutrinos within the active detector volume	Signal directionality and event topology

NEXT STEP: PRELIMINARY

IN A XENON-GAS TPC DETECTOR WITH BARIUM-TAGGING CAPABILITY

Discrimination performances